

DEADLY ULTRAVIOLET UV-C AND UV-B

PENETRATION TO EARTH'S SURFACE:

HUMAN AND ENVIRONMENTAL HEALTH

IMPLICATIONS

ABSTRACT

Aims: The dangerous portion of ultraviolet radiation is widely believed to be completely absorbed by the atmosphere before reaching Earth's surface. Our objective is to make multiple measurements at Earth's surface of the solar irradiance spectrum in the range 200-400 nm.

Methods: We made numerous measurements of the solar irradiance spectrum in the range 200-400 nm at an elevation of 56 m with International Light Technologies ILT950UV Spectral Radiometer mounted on a Meade LXD55 auto guider telescope tripod and mount assembly.

Results: Our multifold measurements of solar irradiance spectra demonstrate conclusively that all wavelengths in the spectral range 200-400 nm reach Earth's surface, contrary to the widespread perception that all UV-C and the majority of UV-B never reach the surface. We confirm the surface UV-C measurements of D'Antoni et al. (2007) that were disputed, based on faulty computer model calculations of atmospheric ozone, and thereafter ignored by the geoscience community.

Conclusions: The veracity of our data and D'Antoni et al. (2007)'s data call into question the validity of atmospheric ozone models. Further, we call into question the simplistic supposition of the Montreal Protocol that chloro-fluoro-hydrocarbons are the primary cause of ozone depletion, and point to the very heavy burden of halogens introduced into the atmosphere by ongoing jet-sprayed coal-fly-ash geoengineering. We demonstrate that satellite-based LISIRD solar spectra irradiance at the top of the atmosphere is badly flawed with some regions of the spectrum being less intense than measured at Earth's surface. That calls into question any calculations made utilizing LISIRD data. We provide introductory information on the devastating effects of UV-B and UV-C on humans, phytoplankton, coral, insects and plants. These will be discussed in greater detail in subsequent articles.

Keywords: ultraviolet measurement, UV-C, UV-B, LISIRD, ozone depletion, ozone, ultraviolet damage, ultraviolet harm

1. INTRODUCTION

Geoengineering may be defined as the deliberate large-scale manipulation of the planetary environment including, but not limited to, dispersing particulate matter into the atmosphere to alter climate [1]. Geoengineering experiments, conducted by the U. S. military and involving particulates emplaced into the atmosphere, dates back to 1958 [2] and have continually increased in intensity and geographic range. In approximately the year 2010, presumably through a secret international agreement, jet-spraying of particulates into the atmosphere became near-daily in intensity and near-global in range. The covert aerial particulate spraying was conducted without informed consent of those breathing the contaminated air, but with orchestrated false information, including in the scientific literature [3,4].

The geoscience community and the United Nation's Intergovernmental Panel on Climate Change, IPCC, has misled the public and the scientific community by not taking into account the

27 consequences of aerial particulate spraying on climate [5]. Even those who study the atmosphere do
28 not mention the very-obvious aerial spraying, Figure 1.



29

30 **Figure 1.** Geoengineering aerosol particulate trails across the February 4, 2017 sky in Soddy-Daisy,
31 TN (USA). With permission of David Tulis.

32 The typical geoscience presentation of the case for geoengineering is both simplistic and incorrect: In
33 the future it may be necessary to place substances into the atmosphere to reflect away a portion of
34 incident sunlight, 'sunshades for the Earth'; to compensate for supposed global warming presumably
35 due to anthropogenic greenhouse gases, especially carbon dioxide. Placing particulate matter into the
36 atmosphere not only reflects away a portion of incident sunlight, but also permits the particles to
37 absorb radiant solar energy and transfer it to the atmosphere by molecular collisions. Furthermore,
38 emplaced particulate aerosols retard infrared heat loss from Earth's surface and impede rainfall by
39 preventing moisture droplets from coalescing to become massive enough to fall as rain. Eventually,
40 the atmosphere becomes so moisture-saturated that it results in abnormal downpours, storms, and
41 flooding. In short, the aerial particulate emplacement has a net effect of causing global warming and
42 disrupting normal hydrological cycles.

43 Moreover, as described below (and in subsequent articles in this series), ongoing geoengineering
44 may be causing a disruption of the ozone layer, endangering all life.

45 Though the geoscience community ignores the aerosol particulate spraying, there are many millions
46 of ordinary citizens who harbor legitimate concerns about that activity [6]. Some individuals have
47 taken rainwater samples and had them analyzed by commercial laboratories. Usually aluminum
48 analyses have been requested; sometimes aluminum and barium; and rarely, aluminum, barium and
49 strontium. We had rain and snow samples analyzed for a greater number of elements and showed
50 that the elements thus determined were consistent with coal fly ash as the main aerosolized
51 substance used in ongoing geoengineering operations [7-11].

52 When coal is burned by electric utilities the heavy ash settles and the light ash, called coal fly ash
53 (CFA), forms and accumulates in the hot gases above the burner. Unless trapped and sequestered,
54 the CFA exits the utilities' smokestacks. Coal fly ash contains a concentration of the toxic elements
55 found in coal, including arsenic, chromium, thallium, and radioactive elements, to name a few. Coal fly
56 ash also contains environmentally harmful elements such as mercury and chlorine. For public and
57 environmental health reasons CFA is typically trapped and stored in Western nations.

58 Why would CFA be sprayed into the atmosphere for geoengineering purposes? CFA is one of the
59 world's largest industrial waste streams with approximately 160 million tons generated annually in the
60 U.S. [12], and approximately 750 million tons generated annually worldwide [13]. Little additional

61 processing is necessary for this abundantly available and inexpensive waste product to be utilized in
62 aerosol geoengineering operations as CFA particles typically form in the size range 0.1 – 50 μm [14].
63 Worldwide availability, low cost, and in-place production and storage facilities at coal-burning utilities
64 all contribute to making CFA an attractive aerosol geoengineering material. Though CFA is no longer
65 regulated as a hazardous waste by the U. S. **Environmental Protection Agency**, it is nonetheless toxic
66 to most biota and, as discussed below, disrupts the atmospheric integrity that makes life possible on
67 Earth.

68 Life on Earth depends critically on natural processes that shield it from the relentless hazardous
69 onslaught of solar radiation. The first line of defense is the geomagnetic field that deflects the brunt of
70 the sun's charged particles safely around Earth [15]. Our atmosphere is the second line of defense
71 that protects life from solar ultraviolet radiation. Plants and animals on Earth are shielded from harmful
72 solar radiation by our planet's stratospheric ozone layer, which is thought to form from the interaction
73 of ultraviolet radiation with O_2 , which is produced and sustained by photosynthesizing organisms. On
74 numerous occasions the assertion has been made that no UV-C radiation (100-290 nm) reaches
75 Earth's surface [16-18]. Here we dispute that assertion, using spectrometric measurements that
76 indicate the probable debilitation of Earth's biota caused by the levels of UV-C radiation we recorded
77 over the course of one year.

78 Ozone (O_3) and atmospheric oxygen (O_2) are widely thought to prevent over 90% of the UV-B
79 radiation (290-320 nm) and all of the UV-C radiation (100-290 nm) from reaching Earth's surface. For
80 the past three decades the geoscience community has focused on ozone depletion in connection with
81 the so-called Antarctic 'ozone hole', and held to the theory, adopted by the 1987 Montreal Protocol,
82 that fluoro-chloro-hydrocarbons (CFCs) are primarily responsible for the destruction of ozone through
83 atmospheric reactions that produce ozone-destroying chlorine. Here we dispute that theory and
84 recommend that other sources for ozone depletion should be considered, notably including CFA
85 aerosol geoengineering.

86

87 **2. METHODS**

88

89 The experimental method employed pertains to solar spectrometric irradiance measurements at
90 Earth's surface. This is a new line of investigation employing International Light Technologies
91 ILT950UV Spectral Radiometer with fractional-nanometer resolution in the short-wavelength portion of
92 the ultraviolet (UV) spectrum **with stray light rejection >99.7%**. The initial order to International Light
93 Technologies specified that solar radiation measurements were to be performed with this unit, and
94 that power levels to be measured in $\mu\text{W}/\text{cm}^2/\text{nm}$. International Light Technologies provided all
95 training, and feedback analysis of initial data gathered to insure correct measurement process. The
96 ILT950UV Spectral Radiometer was certified to ISO 17025.

97 The measurement process is as follows: The sensor for the ILT950UV is attached to a bracket located
98 on the forward ring mount of the Meade LXD55 auto guider telescope tripod and mount assembly.
99 The ILT950UV Spectral Radiometer is form fitted with foam rubber and installed inside the mount
100 rings. The sensor and Radiometer are attached via fiber optic cable. This telescope mount is then set
101 to the current latitude, oriented true North, programmed with current date and time, and then allowed
102 to complete a calibration sequence. Post completion of this calibration, Sol is selected and entered.
103 The telescope mount automatically tracks to Sol, and provides an accuracy of +/- 50 arc seconds
104 relative to Sol. This automatic tracking of Sol mitigates the addition of "Sigma" phase error
105 mathematical corrections.

106 The ILT950UV is then attached to a laptop computer with the software provided by International Light
107 Technologies. A USB cable is attached from the laptop computer and the ILT950UV. The assembly is
108 shown in Figure 2.



109

110 **Figure 2.** Spectrometer system.

111 The International Light Technologies software Program is initialized using “Administrator” privileges to
112 ensure primary communication via the USB interface. The dark cap is installed over the sensor on the
113 telescope mount, and the ILT950UV software calibration procedure begins with selecting the
114 calibration file supplied by International Light Technologies, under the “SETUP” function tab.

115 Under the “ACQUIRE” tab, the Integration time is set to 10 milliseconds, and the SCAN AVERAGE is
116 set to 100. The integration time is much like setting the exposure level on a camera, and was selected
117 for “best fit” of high and low irradiance levels, keeping within the dynamic range of the radiometer. The
118 SCAN AVERAGE of 100 allows higher repeatability.

119 Next, a “DARK SCAN” is performed with the dark cap placed over the sensor, the ILT950UV “Dark
120 Scan” is selected under the “Acquire” tab, and when complete responds with a “green” “DARK: ON”
121 (background color of the cell) indication at the bottom center left of the computer display notifying the
122 user the dark reference is valid.

123 The dark cap over the sensor is removed, and under the “Acquire” tab a “Reference Scan” is selected,
124 once complete the ILT950UV validates with a “green” “REF: ON” indication at the bottom center right
125 of the computer display.

126 Once the Dark and Reference scans are complete, the “Timeline” is selected under the “Acquire” tab.
127 Within the GUI that is displayed there is a calendar and time start/stop setting, the interval setting, and
128 how the data is to be exported to a file.

129 Solar position angles relative to the measurement geophysical location determine the length of the
130 data recording session, with winter months being the shortest of 3 to 4 hours, and summer the longest
131 with up to 6 hours.

132 The “Timeline” is set and the interval is set to 2 seconds. This provides a complete spectral scan from
133 200 to 450 nanometers every 2 seconds, and results in 1,854 data points gathered from 200 to
134 450nm in 1 scan, to be repeated every 2 seconds.

135 The “Export as Excel file” button is selected with “TimelineBY_” preceding the date and time code
136 information of each filename used.

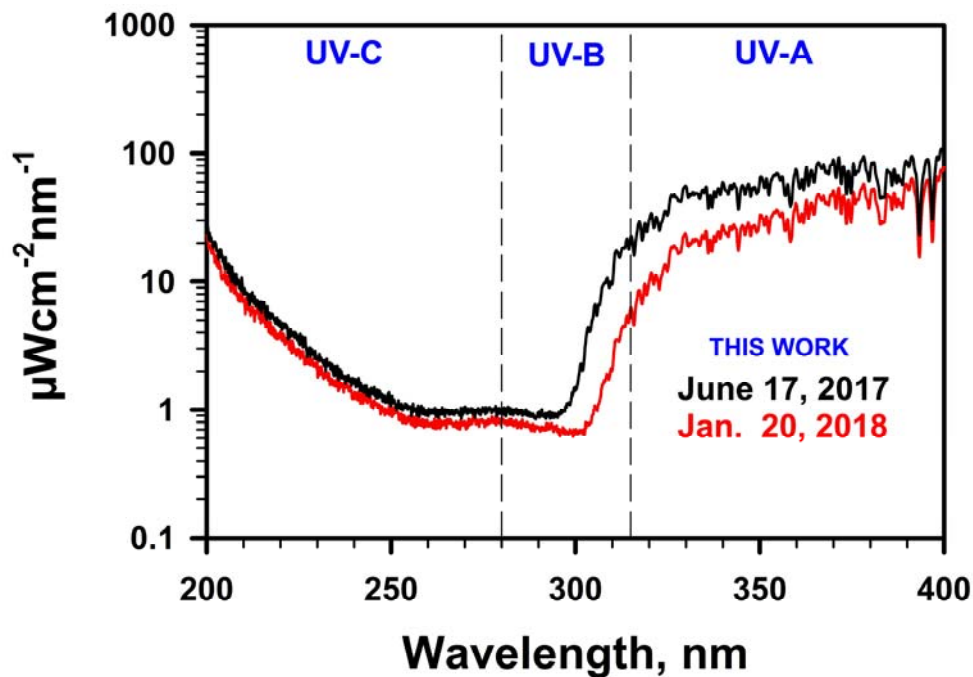
137 Once the “Start” and “Stop” entries are made, the “Begin” button is activated which starts the Spectral
138 Radiometer scans.

139

140 3. RESULTS AND DISCUSSION

141

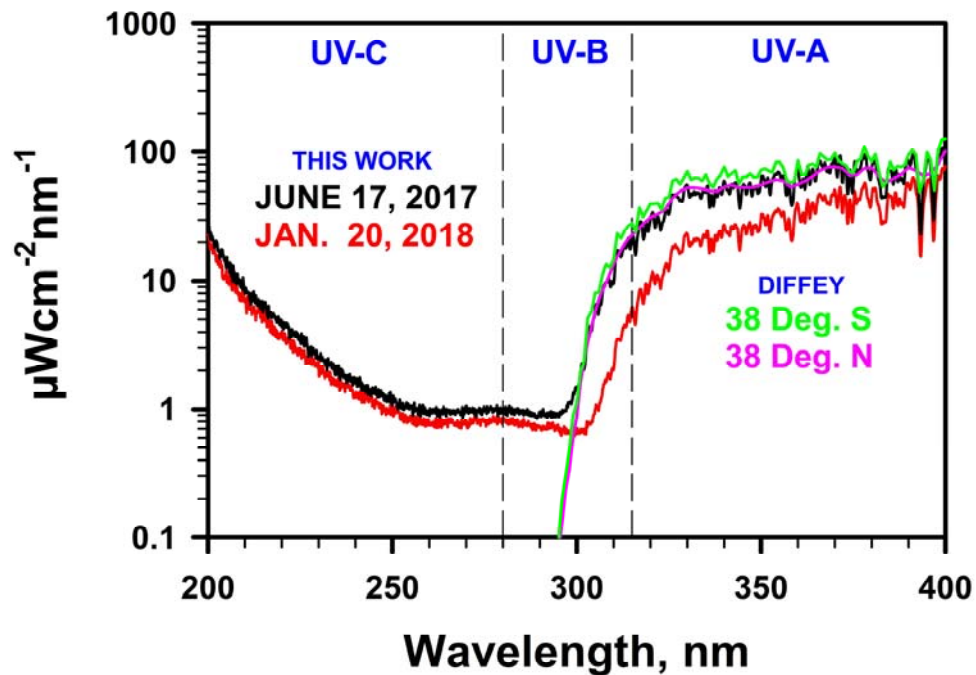
142 The two curves in Figure 3 present typical examples of the spectrometric data obtained using the
143 ILT950UV in the manner described above at 10:49a local time on June 17, 2017 (black curve) at
144 location (37.517783, -120.856783), elevation 56 m and at 12:21p local time on January 20, 2018 (red
145 curve) at the same location. Clearly the spectral irradiances extend throughout the entire ultraviolet
146 (UV) spectrum (200–400 nm) shown. Generally, for purposes of discussion the UV spectrum is
147 divided into three parts, UV-A, UV-B, and UV-C, although some variation exists in wavelength
148 specifications of those divisions. Here we use vertical dashed lines to indicate one set of divisions.



149

150 **Figure 3.** Examples of our solar spectral irradiance measurements.

151 There are widespread assertions in the medical, public health, and geoscience literature that no UV-C
152 reaches the surface and only a portion of the UV-B does so [18-22]. Figure 4 shows our solar spectral
153 irradiance measurements from Figure 3 together with two solar irradiance spectra measured at
154 latitudes 38°S (green curve) and 38°N (pink curve) as reported in 2002 [23]. Close inspection of the
155 figure reveals that the 38°S green curve has higher resolution than the 38°N pink curve, but, more
156 importantly, our red and black curves have even higher resolution than the 38°S green curve. Our
157 higher resolution is particularly important when one notices the major difference in those curves: All of
158 our UV-B and all of our UV-C measurements are non-zero, quite unlike the widespread and incorrect
159 assumption [18-22].

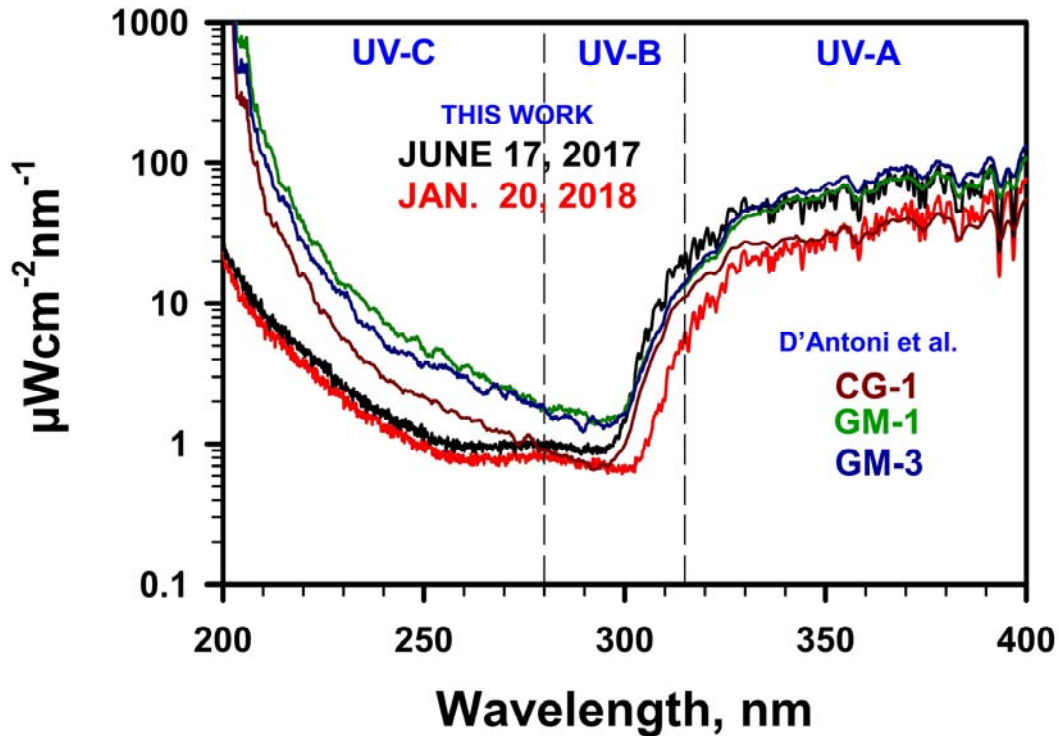


160

161 **Figure 4.** Comparison of our solar spectral irradiance measurements with those of Diffey [22].

162 For more than four decades, the geoscience community has increasingly functioned on the basis of
 163 committee/political standards rather than long-held scientific standards [24]. When an important
 164 contradiction arises in science, scientists have an obligation to attempt to ascertain the veracity of the
 165 contradiction and, if warranted, to correct the contradicted former understanding.

166 **D'Antoni et al. (2007)** [25] published spectral irradiance measurements made on two mountain slopes
 167 in Tierra del Fuego, Argentina with elevations ranging 245-655 m. All of their published results
 168 showed detected radiation in the UV-C region. Figure 5 compares our measured solar spectral
 169 irradiance measurements from Figure 3 with published spectral irradiance measurements of **D'Antoni**
 170 **et al. (2007)** [25].



171

172 **Figure 5.** Comparison of our solar spectrometric measurements with those of **D'Antoni et al. (2007)**
 173 [25]. Note the commonality of shape of the curves in the UV-C region of the spectrum.

174

175 In Figure 5 we provide confirmatory evidence of the veracity of **D'Antoni et al. (2007)**'s measurements,
 176 which in turn confirms our own measurements. Independently, solar UV-C radiation was detected at
 177 Earth's surface using a fundamentally different methodology, employing a KCl:Eu2+ dosimeter
 178 [26,27]. That independent detection of UV-C irradiance stands as evidence that our UV-C
 179 measurements and **D'Antoni et al. (2007)**'s UV-C measurements were not the result of spurious
 180 spectrometer-generated artifacts. The manufacturer of the spectrometer used by **D'Antoni et al.**
 181 **(2007)**, USB 4000, at the time claimed maximum sensitivity in the range 250-400 nm and provided no
 182 calibration data for shorter wavelengths. The manufacturer of the spectrometer we used, ILT950UV,
 183 claims accuracy of $\pm 20\%$ in the range 200-350 nm and $\pm 10\%$ in the range 350-400 nm. After making
 184 the 2018 measurements, shown in Figure 5, the ILT950UV was returned to the manufacturer for
 185 calibration where it was received within manufacture's tolerance specifications of original, new
 186 equipment calibration.

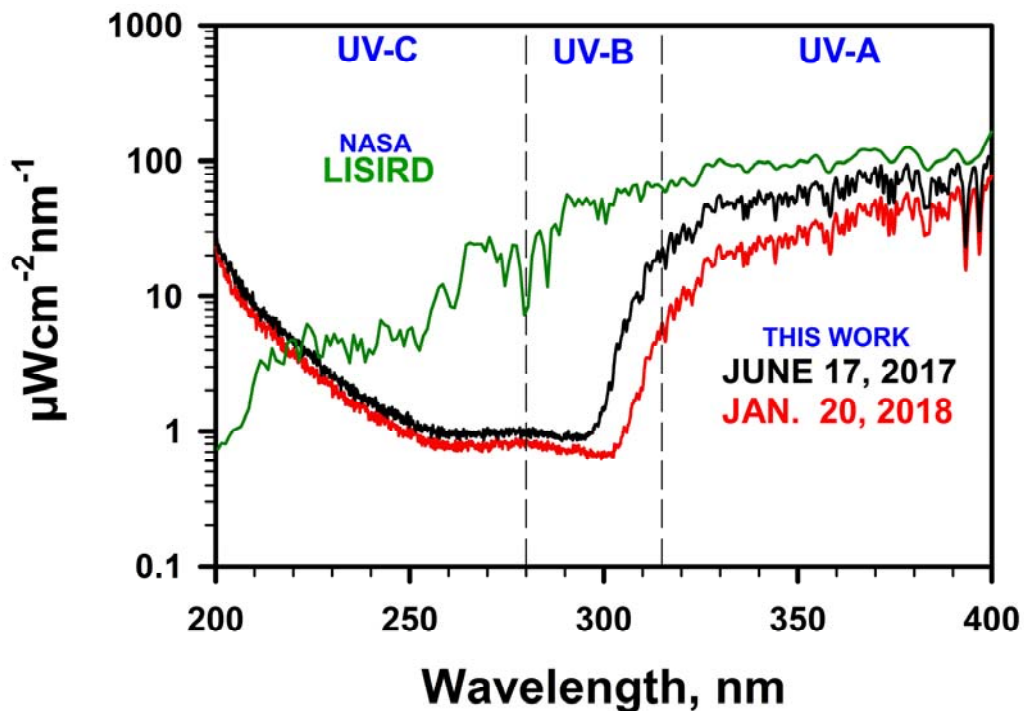
187 **Flint et al. (2008)** [28] published a response to **D'Antoni et al. (2007)** [25] in which they claimed the
 188 measurements were without merit, to which **D'Antoni et al. (2008)** [29] replied. **Flint et al. (2008)**
 189 asserted, **without supporting spectral measurements**, that ozone model calculations ruled out UV-C
 190 reaching Earth's surface, therefore the spectrometer must have been defective. Based upon the data
 191 shown in Figure 5, clearly those model calculations of atmospheric ozone were wrong.

192 Models are not science, they are computer programs that typically begin with a known end result and
 193 achieve that end result by making selective assumptions and parameter choices. During the last four
 194 decades computer-model calculations have burgeoned. It is far easier to make models than to make
 195 basic scientific discoveries, and it is the latter, not the former, that are fundamental to scientific
 196 progress [30].

197 In science when a discovery is made that contradicts current understanding, scientists have the
198 responsibility to attempt to refute the discovery beyond reasonable doubt. If unable to do so, the
199 implications of the new discovery should be discussed in the scientific literature. The discovery by
200 D'Antoni et al. (2007) of UV-C radiation reaching Earth's surface should have been the subject of
201 intense investigation by NASA for two reasons, one scientific and one ethical: Because of its
202 implication for atmospheric science and because of its profound implications for human and
203 environmental health. NASA conducted no follow-up investigation, despite the grave implications of
204 their own measurements. D'Antoni's retirement from NASA shortly after publication was not a factor
205 as the second author has remained employed by NASA. This inaction begs the question: Is NASA
206 complicit in a covert global activity, such as the aerial jet-spraying of toxic coal fly ash that poses
207 serious risks to life on Earth?

208 Our solar spectral measurements and those of D'Antoni et al. (2007) should be repeated objectively
209 and independently throughout the world, throughout ranges of elevations and latitudes and longitudes
210 and atmospheric conditions. Independent scientists can make these measurements since the
211 apparatus we used is commercially available at relatively low-cost (< US\$ 10,000.).

212 In Figure 6 we show our Earth surface solar spectral irradiance data from Figure 3 compared with
213 LISIRD satellite-derived solar spectral irradiance at the top of the atmosphere [31], indicated by the
214 green curve for each of the two dates which are coincident. With satellite-data sets such as this it
215 is difficult to know whether the data is raw or altered based upon models or assumptions. Clearly, there
216 is a problem when the measured ground-level solar UV-C irradiance exceeds that at the top-of-
217 atmosphere.



218

219 **Figure 6.** Comparison of our UV solar spectral irradiance with NASA's LISIRD satellite-derived solar
220 spectral irradiance at the top of the atmosphere [31].

221

222 The consensus-approved, model-driven solar irradiance storyline is badly flawed with regard to ozone
 223 viability and perceived threats to ozone depletion. UV-C and all of UV-B radiation reach Earth's
 224 surface where they pose potentially serious environmental and human health problems. The Montreal
 225 Protocol prohibition of CFCs does not begin to address the life-threatening problems posed by other
 226 sources of ozone-destroying chemicals. Table 1 shows the range of halogen compositions of coal fly
 227 ash (CFA). Covert geoengineering that jet-sprays massive quantities of ultra-fine CFA potentially
 228 places vast amounts of chlorine, bromine, fluorine and iodine into the atmosphere all of which can
 229 deplete ozone. Potentially other substances in CFA aerosols, including nano-particulates, might
 230 adversely affect atmospheric ozone.

231

232 **Table 1.** Range of halogen element compositions of CFA [32]

Chlorine	Bromine	Fluorine	Iodine
µg/g	µg/g	µg/g	µg/g
13 – 25,000	0.3 – 670	0.4 – 624	0.1 – 200

233

234 Ultraviolet radiation is the most harmful and genotoxic component of the solar radiation spectrum.
 235 The mutagenicity and lethal action of sunlight exhibit two maxima, both in the UV region of the
 236 spectrum. This is because DNA bases can directly absorb incident UV photons of certain
 237 wavelengths. Solar radiation can give rise to cellular DNA damage by either (1) direct excitation of
 238 DNA (UV-B and UV-C) or (2) indirect mechanisms that involve excitation of other cellular
 239 chromophores acting as endogenous photosensitizers (UV-A) [33]. The direct excitation of DNA
 240 generates predominantly cyclobutane pyrimidine dimers and photoproducts, which are of principal
 241 importance for the cytotoxic, mutagenic, and carcinogenic effects of short-wave UV radiation (UV-B
 242 and UV-C) [34]. Some of the most hazardous UV radiations have wavelengths between 240 and 300
 243 nm. In this range, the wavelength with the minimum TLV (threshold limit value), or most hazardous, is
 244 around 270 nm [35].

245 UV-B radiation is a global stressor with potentially far-reaching ecological impacts. A meta-analysis of
 246 UV radiation on marine and freshwater organisms found large negative (but variable) effects of UV-B
 247 on survival and growth of organisms that crossed life histories, trophic groups, habitats, and life
 248 history stages [36]. In phytoplankton and zooplankton, increased levels of UV-B can affect
 249 photosynthesis, decrease growth and metabolic rates, impair nitrogen assimilation, impair motility,
 250 and bleach photopigments [37]. Extreme UV-B radiation is damaging to coral reef communities and
 251 associated with coral bleaching processes [38]. Corals accidentally exposed to UV-C showed
 252 gastrodermal cell death and necrosis resulting in the release of intracellular zoo-xanthellae into the
 253 gastrovascular canals and water column, likely resulting in a bleaching effect [39].

254 Enhanced UV-B radiation reduces genome stability in plants [40]. Enhanced UV radiation affects
 255 trees by direct action and modification of their biological/chemical environment (Figure 7). A recent
 256 study documents that high UV-B intensity leads to defective pollen development in conifers and
 257 decreased reproductive success or even sterilization [41].



258

259 **Figure 7.** July 21, 2017 photo of tree in New York, NY (USA) showing UV burn and concomitant
260 fungal growth on sun-exposed side.

261 The toxicity of UV-C (100-280 nm) is well known. UV-C irradiation has lethal effects on insects and
262 microorganisms [42,43]. UV-C radiation induces programmed cell death, or apoptosis, in plant cells
263 [44]. In a controlled study, numerous ultrastructural changes and associated cell damage were shown
264 in mole rat kidney tissue cells irradiated with artificially produced UV-C radiation [45]. Medical
265 students accidentally exposed for 90 minutes to UV-C radiation from a germicidal lamp all suffered
266 reversible photokeratitis, and skin damage to the face, scalp, and neck [46].

267

268 **4. CONCLUSION**

269

270 Measurement of solar irradiance spectra in the range 200-400 nm demonstrates conclusively that all
271 wavelengths in that spectral range reach Earth's surface, contrary to the widespread perception that
272 all UV-C and the majority of UV-B never reaches the surface. We confirm the 2007 surface UV-C
273 measurements of [D'Antoni et al. \(2007\)](#) that were disputed, based on faulty computer model
274 calculations of atmospheric ozone, and thereafter ignored by the geoscience community. The veracity
275 of [D'Antoni et al. \(2007\)](#)'s data call into question the validity of atmospheric ozone models. Further, we
276 call into question the simplistic supposition of the Montreal Protocol that CFCs are the primary cause
277 of ozone depletion, and point to the very heavy burden of halogens introduced into the atmosphere by
278 ongoing jet-sprayed coal-fly-ash geengineering. We demonstrate that LISIRD solar spectra
279 irradiance at the top of the atmosphere is badly flawed with some regions of the spectrum being less
280 intense than measured at Earth's surface. That calls into question any calculations made utilizing

281 LISIRD data. We provided introductory information on the **devastating** effects of UV-B and UV-C on
282 humans, phytoplankton, coral, insects and plants. These will be discussed in **greater** detail in
283 subsequent articles.

284

285 **ACKNOWLEDGEMENTS**

286

287 We thank Dr. Hector L. D'Antoni for sharing the raw data from his important 2007 report on
288 measurement of solar UV-C radiation at Earth's surface. We are grateful to Environmental Voices and
289 its donors for providing funds for laboratory and publication fees. We thank GeoengineeringWatch for
290 locating an individual whose gift, along with other contributions, in part made possible the UV-C
291 detection system.

292

293

294 **Authors' Ethical Statement:**

295

296 The authors hold that technical, scientific, medical, and public health representations made in the
297 scientific literature in general, including this particular journal, should be and are truthful and accurate
298 to the greatest extent possible, and should serve to the highest degree possible to protect the health
299 and well-being of humanity and Earth's natural environment.

300

301 **Ethical Approval:**

302

303 As per international standard or university standard written ethical approval has been collected and
304 preserved by the author(s).

305

306

307

308 **REFERENCES**

309

310 1. Shepherd J, Caldeira K, Cox P, Haigh J, Keith D, Launder B, et al. Geoengineering the
311 Climate: Science, Governance and Uncertainty 2009. Royal Society: London.

312

313 2. <http://www.nuclearplanet.com/1958evidence.pdf> Accessed March 10, 2018.

314

315 3. Shearer C, West M, Caldeira K, Davis SJ. Quantifying expert consensus against the
316 existence of a secret large-scale atmospheric spraying program. Environ Res Lett. 2016;11(8):p.
317 084011.

318

319 4. Tingley D, Wagner G. Solar geoengineering and the chemtrails conspiracy on social media.
320 Palgrave Communications. 2017;3(1):12.

321

322 5. Herndon JM. An open letter to members of AGU, EGU, and IPCC alleging promotion of fake
323 science at the expense of human and environmental health and comments on AGU draft
324 geoengineering position statement. New Concepts in Global Tectonics Journal. 2017;5(3):413-6.

325

326 6. <http://wwwnuclearplanetcom/websites.pdf> Accessed March 10, Accessed March 10, 2018.

327

- 328 7. Herndon JM. Aluminum poisoning of humanity and Earth's biota by clandestine
329 geoengineering activity: implications for India. *Curr Sci*. 2015;108(12):2173-7.
- 330
- 331 8. Herndon JM. Obtaining evidence of coal fly ash content in weather modification
332 (geoengineering) through analyses of post-aerosol spraying rainwater and solid substances. *Ind J Sci*
333 *Res and Tech*. 2016;4(1):30-6.
- 334
- 335 9. Herndon JM. Adverse agricultural consequences of weather modification. *AGRIVITA Journal*
336 *of agricultural science*. 2016;38(3):213-21.
- 337
- 338 10. Herndon JM, Whiteside M. Further evidence of coal fly ash utilization in tropospheric
339 geoengineering: Implications on human and environmental health. *J Geog Environ Earth Sci Intn*.
340 2017;9(1):1-8.
- 341
- 342 11. Herndon JM, Whiteside M. Contamination of the biosphere with mercury: Another potential
343 consequence of on-going climate manipulation using aerosolized coal fly ash *J Geog Environ Earth*
344 *Sci Intn*. 2017;13(1):1-11.
- 345
- 346 12. Yao Z, Ji X, Sarker P, Tang J, Ge L, Xia M, et al. A comprehensive review on the applications
347 of coal fly ash. *Earth-Science Reviews*. 2015;141:105-21.
- 348
- 349 13. Izquierdo M, Querol X. Leaching behavior of elements from coal combustion fly ash: an
350 overview. *Int J Coal Geol*. 2012;94:54-66.
- 351
- 352 14. Chen Y, Shah N, Huggins F, Huffman G, Dozier A. Characterization of ultrafine coal fly ash
353 particles by energy filtered TEM. *Journal of Microscopy*. 2005;217(3):225-34.
- 354
- 355 15. Parker E. Interaction of the solar wind with the geomagnetic field. *The Physics of Fluids*.
356 1958;1(3):171-87.
- 357
- 358 16. Frederick J, Snell H, Haywood E. Solar ultraviolet radiation at the earth's surface.
359 *Photochemistry and photobiology*. 1989;50(4):443-50.
- 360
- 361 17. Pinedo-Vega JL, Ríos-Martínez C, Navarro-Solís DJ, Dávila-Rangel JI, Mireles-García F,
362 Saucedo-Anaya SA, et al. Attenuation of UV-C Solar Radiation as a Function of Altitude ($0 \leq z \leq 100$
363 km): Rayleigh Diffusion and Photo Dissociation of O₂ Influence. *Atmospheric and Climate Sciences*.
364 2017;7(04):540.
- 365

- 366 18. Wilson BD, Moon S, Armstrong F. Comprehensive review of ultraviolet radiation and the
367 current status on sunscreens. *The Journal of clinical and aesthetic dermatology*. 2012;5(9):18.
- 368
- 369 19. Seebode C, Lehmann J, Emmert S. Photocarcinogenesis and skin cancer prevention
370 strategies. *Anticancer research*. 2016;36(3):1371-8.
- 371
- 372 20. Stapleton AE. Ultraviolet radiation and plants: burning questions. *The Plant Cell*.
373 1992;4(11):1353.
- 374 21. <https://www.cdc.gov/healthyouth/skincancer/pdf/ga.pdf>
- 375
- 376 22. <http://www.who.int/uv/faq/whatisuv/en/index2.html>
- 377
- 378 23. Diffey BL. Sources and measurement of ultraviolet radiation. *Methods*. 2002;28(1):4-13.
- 379
- 380 24. Herndon JM. Corruption of Science in America. *The Dot Connector*. 2011.
381 <http://www.nuclearplanet.com/corruption.pdf>
- 382
- 383 25. D'Antoni H, Rothschild L, Schultz C, Burgess S, Skiles J. Extreme environments in the forests
384 of Ushuaia, Argentina. *Geophysical Research Letters*. 2007;34(22).
- 385
- 386 26. Córdoba C, Muñoz J, Cachorro V, de Cárcer IA, Cussó F, Jaque F. The detection of solar
387 ultraviolet-C radiation using KCl:Eu²⁺ thermoluminescence dosimeters. *Journal of Physics D:
388 Applied Physics*. 1997;30(21):3024.
- 389
- 390 27. de Cárcer IA, D'Antoni H, Barboza-Flores M, Correcher V, Jaque F. KCl: Eu²⁺ as a solar UV-
391 C radiation dosimeter. Optically stimulated luminescence and thermoluminescence analyses. *Journal
392 of Rare Earths*. 2009;27(4):579-83.
- 393
- 394 28. Flint SD, Ballaré CL, Caldwell MM, McKenzie RL. Comment on "Extreme environments in the
395 forests of Ushuaia, Argentina" by Hector D'Antoni et al. *Geophysical Research Letters*. 2008;35(13).
- 396
- 397 29. D'Antoni HL, Rothschild LJ, Skiles J. Reply to comment by Stephan D. Flint et al. on "Extreme
398 environments in the forests of Ushuaia, Argentina". *Geophysical Research Letters*. 2008;35(13).
- 399
- 400 30. Herndon JM. Geodynamic Basis of Heat Transport in the Earth. *Curr Sci*. 2011;101(11):1440-
401 50.

402

403 31. LISIRD Data Systems Group, 2017, LASP Interactive Solar Irradiance Dataset,
404 <http://lasp.colorado.edu/lisird/lya/>

405

406 32. NRC. Trace-element Geochemistry of Coal Resource Development Related to Environmental
407 Quality and Health: National Academy Press; 1980.

408

409 33. Ravanat J-L, Douki T, Cadet J. Direct and indirect effects of UV radiation on DNA and its
410 components. *Journal of Photochemistry and Photobiology B: Biology*. 2001;63(1):88-102.

411

412 34. Kielbassa C, Roza L, Epe B. Wavelength dependence of oxidative DNA damage induced by
413 UV and visible light. *Carcinogenesis*. 1997;18(4):811-6.

414

415 35. http://www2.lbl.gov/ehs/safety/nir/ultraviolet_radiation.shtml

416

417 36. Bancroft BA, Baker NJ, Blaustein AR. Effects of UVB radiation on marine and freshwater
418 organisms: a synthesis through meta-analysis. *Ecology letters*. 2007;10(4):332-45.

419

420 37. El-Sayed SZ, Van Dijken GL, Gonzalez-Rodas G. Effects of ultraviolet radiation on marine
421 ecosystems. *International Journal of Environmental Studies*. 1996;51(3):199-216.

422

423 38. Lyons M, Aas P, Pakulski J, Van Waasbergen L, Miller RV, Mitchell D, et al. DNA damage
424 induced by ultraviolet radiation in coral-reef microbial communities. *Marine Biology*. 1998;130(3):537-
425 43.

426

427 39. Basti D, Bricknell I, Beane D, Bouchard D. Recovery from a near-lethal exposure to
428 ultraviolet-C radiation in a scleractinian coral. *Journal of invertebrate pathology*. 2009;101(1):43-8.

429

430 40. Ries G, Heller W, Puchta H, Sandermann H, Seidlitz HK, Hohn B. Elevated UV-B radiation
431 reduces genome stability in plants. *Nature*. 2000;406(6791):98.

432

433 41. Benca JP, Duijnste IA, Looy CV. UV-B-induced forest sterility: Implications of ozone shield
434 failure in Earth's largest extinction. *Science Advances*. 2018;4(2):e1700618.

435

436 42. Hori M, Shibuya K, Sato M, Saito Y. Lethal effects of short-wavelength visible light on insects.
437 *Scientific Reports*. 2014;4:7383.

438

439 43. Reed NG. The history of ultraviolet germicidal irradiation for air disinfection. Public health
440 reports. 2010;125(1):15-27.

441

442 44. Danon A, Gallois P. UV-C radiation induces apoptotic-like changes in *Arabidopsis thaliana*.
443 FEBS letters. 1998;437(1-2):131-6.

444

445 45. Türker H, Yel M. Effects of ultraviolet radiation on mole rats kidney: A histopathologic and
446 ultrastructural study. Journal of Radiation Research and Applied Sciences. 2014;7(2):182-7.

447

448 46. Trevisan A, Piovesan S, Leonardi A, Bertocco M, Nicolosi P, Pelizzo MG, et al. Unusual High
449 Exposure to Ultraviolet-C Radiation. Photochemistry and photobiology. 2006;82(4):1077-9.